

## An Analytical Model for the Two-Scalar Covariance Budget Inside a Uniform Dense Canopy

Gabriel G. Katul · Daniela Cava · Samuli Launiainen ·  
Timo Vesala

Received: 25 June 2008 / Accepted: 5 February 2009 / Published online: 24 February 2009  
© Springer Science+Business Media B.V. 2009

**Abstract** The two-scalar covariance budget is significant within the canopy sublayer (CSL) given its role in modelling scalar flux budgets using higher-order closure principles and in estimating the segregation ratio for chemically reactive species. Despite its importance, an explicit expression describing how the two-scalar covariance is modified by inhomogeneity in the flow statistics and in the vertical variation in scalar emission or uptake rates within the canopy volume remains elusive even for passive scalars. To progress on a narrower version of this problem, an analytical solution to the two-scalar covariance budget in the CSL is proposed for the most idealized flow conditions: a stationary and planar homogeneous flow inside a uniform and dense canopy with a constant leaf area density distribution. The foliage emission (or uptake) source strengths are assumed to vary exponentially with depth while the forest floor emission is represented as a scalar flux. The analytical solution is a superposition of a homogeneous part that describes how the two-scalar covariance at the canopy top is transported and dissipated within the canopy volume, and an inhomogeneous part governed by local production mechanisms of the two-scalar covariance. The homogeneous part is primarily described by the canopy adjustment length scale, and the attenuation coefficients of the turbulent kinetic energy and the mean velocity. Conditions for which the vertical variation

---

G. G. Katul (✉)  
Nicholas School of the Environment, Duke University, Box 90328, Durham, NC 27708-0328, USA  
e-mail: gaby@duke.edu

G. G. Katul  
Department of Civil and Environmental Engineering, Duke University, Durham, NC 27708-0328, USA

D. Cava  
CNR—Institute of Atmosphere Sciences and Climate U.O. of Lecce, Lecce, Italy  
e-mail: d.cava@isac.cnr.it

S. Launiainen · T. Vesala  
Department of Physics, University of Helsinki, P.O. Box 64, 00014 Helsinki, Finland  
e-mail: samuli.launiainen@helsinki.fi

T. Vesala  
e-mail: Timo.Vesala@helsinki.fi

of the two-scalar covariance is controlled by the rapid attenuation in the mean velocity and turbulent kinetic energy profiles, vis-à-vis the vertical variation of the scalar source strength, are explicitly established. This model also demonstrates how dissimilarity in the emissions from the ground, even for the extreme binary case with one scalar turned ‘on’ and the other scalar turned ‘off’, modifies the vertical variation of the two-scalar covariance within the CSL. To assess its applicability to field conditions, the analytical model predictions were compared with observations made at two different forest types—a sparse pine forest at the Hyytiälä SMEAR II-station (in Finland) and a dense alpine hardwood forest at Lavarone (in Italy). While the model assumptions do not represent the precise canopy morphology, attenuation properties of the turbulent kinetic energy and the mean velocity, observed mixing length, and scalar source attenuation properties for these two forest types, good agreement was found between measured and modelled two scalar covariances for multiple scalars and for the triple moments at the Hyytiälä site.

**Keywords** Canopy sublayer · Canopy turbulence · Hyytiälä SMEAR II-station · Lavarone field station · Scalar dissimilarity · Scalar transport · Two-scalar covariance budget

## 1 Introduction

When two scalars are emitted from two distinct sources positioned in the same turbulent flow, scalar fluctuations are efficiently mixed yet their combined scalar variance (i.e.  $\overline{(s'_1 + s'_2)^2}$ ) does not only depend on the sum of the individual scalar fluctuation variances (i.e.  $\overline{(s'_1)^2} + \overline{(s'_2)^2}$ ) but also on the covariance between them (i.e.  $2\overline{s'_1 s'_2}$ ), where  $s_1$  and  $s_2$  are concentrations of scalar  $s$  emitted from sources 1 and 2, respectively, the overbar represents a time average, and primed quantities are turbulent excursions from the averaged quantities. It is for this reason that the so-called two-scalar covariance budget has received significant attention in engineering and atmospheric dynamics over the last 30 years (Warhaft 1981; Sirivat and Warhaft 1982). Historically, the research focus in the atmospheric surface layer (ASL) and in the mixed layer (ML) has been on the covariance budget between air temperature ( $T$ ) and water vapour concentration ( $q$ ) fluctuations, primarily because these two scalars jointly modify the radio refractive index and other electromagnetic wave propagation properties (Friehe et al. 1975; Wesely 1976; Wyngaard 1978; Coulman 1980; Sempreviva and Hojstrup 1998; Asanuma et al. 2007; Katul et al. 2008). More recently, the two-scalar covariance budget has received closer attention in the canopy sublayer (CSL) because (1) higher-order closure modelling of scalar flux budgets (i.e. turbulent budgets of the form  $\partial \overline{w's'}/\partial t = \dots$ ) are employed in quantifying biosphere-atmosphere exchange, and these models do require estimates of terms such as  $(g/T) \overline{T's'}$  (Meyers and Paw 1987; Siqueira and Katul 2002; Cava et al. 2006; Juang et al. 2006, 2008), and (2) a priori estimates of segregation ratios  $= \overline{s'_a s'_b} / (\overline{s_a} \overline{s_b})$  are needed when coupling turbulent transport and second-order chemically reactive scalars emitted within the canopy volume (Gao et al. 1993; Gao and Wesely 1994; Patton et al. 2001, among others). Here,  $t$  is time,  $g$  is the gravitational acceleration,  $w$  is the vertical velocity,  $s$  is an arbitrary scalar concentration,  $s_a$  and  $s_b$  are reactive species experiencing second-order chemical interactions, the overbar for within-canopy flows indicates time and space averaging (Raupach and Shaw 1982), and primed quantities are turbulent excursions from such space-time averaged quantities. In applications, scalar emissions (or uptake) from the foliage and the ground must be explicitly included in the two-scalar

covariance budget. To date, there is no simplified or explicit expression illustrating how these scalar emissions (or sinks) from the canopy modify the two-scalar covariance budget, the subject of this work. A number of studies in forested and urban canopies have provided phenomenological models or scaling arguments on how variations in scalar sources affect correlations between two scalars (Roth and Oke 1995; Lamaud and Irvine 2006; Moriwaki and Kanda 2006; Williams et al. 2007; Thomas et al. 2008) though no vertically explicit relationship has been presented.

To make progress on this problem, an analytical solution to the two-scalar covariance budget is proposed for the most idealized conditions in the CSL: a stationary and planar homogeneous flow inside a uniform and dense canopy with a constant leaf area density distribution. For this idealized set-up, the physiological source strengths are assumed to decay exponentially inside the canopy reflecting near-exponential light attenuation and concomitant linear stomatal responses to below-saturation light levels. Hence, it should be emphasized here that the proposed analytical solution does not provide finality to this problem but does provide first-order estimates of the two-scalar covariance magnitude. For notational convenience, it is assumed that one of the scalars is  $T$ , while the other is an arbitrary scalar  $s$  (e.g.  $q$ ), and hereafter, we refer to the two-scalar covariance as  $\overline{T's'}$ . Within the analytical framework proposed here, formulating conditions in which profiles of  $\overline{T's'}$  are primarily controlled by inhomogeneity in the flow statistics vis-à-vis vertical inhomogeneity by the scalar emissions from the canopy are presented assuming that the turbulent kinetic energy and mean velocity also decay exponentially within the canopy.

## 2 Theory

The budget equation for  $\overline{T's'}$  in a stationary and planar homogeneous high Reynolds number and Peclet number flows, in the absence of subsidence, reduces to (Stull 1988; Garratt 1992; Sempreviva and Hojstrup 1998; Juang et al. 2006)

$$\frac{\partial \overline{T's'}}{\partial t} = 0 = - \left( \overline{w's'} \frac{\partial \overline{T}}{\partial z} + \overline{w'T'} \frac{\partial \overline{s}}{\partial z} \right) - 2\varepsilon_{Ts} - \frac{\partial \overline{w'T's'}}{\partial z}, \tag{1}$$

where the first term on the right-hand side is the production term (i.e. term responsible for co-variances between the two scalars), the second term is the dissipation rate, and the third term is the turbulent flux-transport term of  $\overline{T's'}$ . Using standard closure models for the dissipation, given by

$$\varepsilon_{Ts} = \frac{Q}{\lambda_3} \overline{T's'}, \tag{2}$$

and the flux-transport term, given by

$$\overline{w'T's'} = -Q\lambda_1 \frac{\partial \overline{T's'}}{\partial z}, \tag{3}$$

results in a second-order ordinary differential equation (ODE) for the vertical variations of  $\overline{T's'}$

$$\lambda_1 Q \frac{\partial^2 (\overline{T's'})}{\partial z \partial z} + \frac{\partial (\lambda_1 Q)}{\partial z} \frac{\partial \overline{T's'}}{\partial z} - \frac{2}{\lambda_3} Q \overline{T's'} = \left( \overline{w's'} \frac{\partial \overline{T}}{\partial z} + \overline{w'T'} \frac{\partial \overline{s}}{\partial z} \right), \tag{4}$$

where  $Q = \sqrt{u'_i u'_i}$  is a turbulent velocity scale related to the availability of turbulent kinetic energy,  $\lambda_1 = a_1 l_m$  and  $\lambda_3 = a_3 l_m$  are related to the canonical mixing length  $l_m$  inside the canopy, which is assumed constant given by  $l_m = 2\beta_u^3 L_c$ , in a uniform and dense canopy, with  $\beta_u = u_*/U$  defined at the canopy top ( $z/h = 1$ ),  $u_*$  is the friction velocity,  $U$  is the mean velocity,  $L_c = (C_d a)^{-1}$  is the adjustment length,  $C_d$  is the foliage drag coefficient, and  $a = LAI/h$  is the mean leaf area density,  $LAI$  is the leaf area index, and  $h$  is the canopy height (Finnigan and Belcher 2004; Katul et al. 2006).

For analytical tractability, first-order closure principles are employed only to link the mean scalar gradients to turbulent fluxes in some of the production terms to yield

$$\frac{\partial \bar{T}}{\partial z} = \frac{-\overline{w'T'}}{K_{t,T}}, \tag{5a}$$

$$\frac{\partial \bar{s}}{\partial z} = \frac{-\overline{w's'}}{K_{t,s}}, \tag{5b}$$

where  $K_t$  is the turbulent diffusivity, and for the simplest case when  $K_{t,s} = K_{t,T}$ , the  $\overline{T's'}$  budget equation reduces to

$$\frac{\partial^2 (\overline{T's'})}{\partial z \partial z} + \frac{1}{Q} \frac{\partial(Q)}{\partial z} \frac{\partial \overline{T's'}}{\partial z} - \frac{2}{\lambda_1 \lambda_3} \overline{T's'} = -\frac{2}{\lambda_1} \left( \frac{\overline{w's'} \overline{w'T'}}{K_t Q} \right) = P_d(z), \tag{6}$$

where  $P_d(z)$  is a normalized production term. For chemically non-reactive scalars, the mean scalar continuity equation for a stationary and planar homogeneous flow in the absence of subsidence is given by

$$\overline{w's'}(z) = F_s(0) + \int_0^z S_s(z) dz; \quad \overline{w'T'}(z) = F_T(0) + \int_0^z S_T(z) dz, \tag{7}$$

resulting in

$$\begin{aligned} & \frac{\partial^2 (\overline{T's'})}{\partial z \partial z} + \frac{1}{Q} \frac{\partial(Q)}{\partial z} \frac{\partial \overline{T's'}}{\partial z} - \frac{2}{\lambda_3 \lambda_1} \overline{T's'} \\ &= -\frac{2}{K_T \lambda_1 Q} \left( F_s(0) F_T(0) + F_s(0) \int_0^z S_T(z) dz + F_T(0) \int_0^z S_s(z) dz \right. \\ & \quad \left. + \int_0^z S_s(z) dz \int_0^z S_T(z) dz \right). \end{aligned} \tag{8}$$

This expression shows how the local sources and sinks within the canopy and the ground fluxes affect  $P_d$  and subsequently  $\overline{T's'}$  provided the closure constants  $a_1$  and  $a_3$  and appropriate boundary conditions are specified.

### 3 Analytical Solution

An analytical solution for the second-order ODE above can be derived for several cases of  $Q$  and  $S$  vertical shapes. This is explored below.

### 3.1 Homogeneous Solution (i.e. $P_d = 0$ )

Assuming  $Q = Q_o \exp(\beta_Q(z - h))$  and noting that  $Q^{-1}dQ/dz = \beta_Q$  results in a homogeneous solution of the form:

$$\overline{T's'_h}(z) = \left( A_1 + A_2 \exp\left(\frac{B_1}{B_2}z\right) \right) \exp\left(-\frac{1}{2}z\left(\beta_Q - \frac{B_1}{B_2}\right)\right), \tag{9}$$

where  $A_1$  and  $A_2$  are integration constants that must be determined from boundary conditions,  $B_1 = \sqrt{8 + (\beta_Q B_2)^2}$  and  $B_2 = \sqrt{a_1 a_3 l_m^2}$ . These constants do have physical interpretations, with  $B_2$  being the geometric average of the two mixing lengths responsible for flux transport and dissipation, which only varies with  $L_c$  and  $\beta_u$ . However,  $B_1$  varies from a near-constant ( $= \sqrt{8}$ ) when  $\beta_Q \rightarrow 0$  to  $\beta_Q B_2$  when  $\beta_Q$  is very large. If the boundary conditions imposed on the homogeneous ODE are  $\overline{T's'_H}(h)$  at  $z/h = 1$  and  $d\overline{T's'_H}/dz = 0$  at  $z/h = 0$ , then  $A_1$  and  $A_2$  can be evaluated to yield

$$\frac{\overline{T's'_H}(z)}{\overline{T's'_H}(h)} = \sqrt{\frac{Q_o}{Q(z)}} \Psi(z), \tag{10a}$$

$$\Psi(z) = \frac{B_1 \cosh\left(\frac{B_1}{2B_2}z\right) + B_2 \beta_Q \sinh\left(\frac{B_1}{2B_2}z\right)}{B_1 \cosh\left(\frac{B_1}{2B_2}h\right) + B_2 \beta_Q \sinh\left(\frac{B_1}{2B_2}h\right)}. \tag{10b}$$

Note that, with decreasing  $z/h$  (i.e. progressing from canopy top to forest floor), the homogeneous solution is controlled by the product of two opposing exponential terms—an increasing  $(Q_o/Q)^{1/2}$  that scales as  $\exp((1/2)\beta_Q(h - z))$  and a decreasing  $\Psi(z)$  that roughly scales as  $\exp(-(1/2)(B_1/B_2)(h - z))$ . Because

$$\frac{B_1}{2B_2} = \sqrt{\frac{2}{B_2^2} + \frac{1}{4}\beta_Q^2} > \frac{1}{2}\beta_Q, \tag{11}$$

$\Psi(z)$  always decays faster than any increases in  $(Q_o/Q)^{1/2}$  for a decreasing  $z/h$ . Hence, the homogeneous solution suggests that a covariance  $\overline{T's'_H}(h)$  produced at the canopy top must be monotonically attenuated inside the canopy, at least for the boundary conditions specified here. This attenuation is not surprising as the homogeneous solution physically reflects the simultaneous effects of transporting and dissipating within the canopy volume the covariance imposed by the upper boundary condition  $\overline{T's'_H}(h)$ .

### 3.2 General Solution

When the mean velocity profile inside the canopy decays as (Inoue 1963; Saito 1964; Cionco 1965; Massman and Weil 1999; Finnigan and Belcher 2004)

$$U(z) = U_o \exp\left(\frac{\beta_u}{l_m}(z - h)\right) = \frac{u_*}{\beta_u} \exp\left(\frac{\beta_u}{l_m}(z - h)\right), \tag{12}$$

the turbulent diffusivity must also decay as

$$K_t = l_m^2 \left| \frac{\partial U}{\partial z} \right| = l_m u_* \exp\left(\frac{\beta_u}{l_m}(z - h)\right) \tag{13}$$

when the turbulent Schmidt number (ratio of scalar to momentum turbulent diffusivity) is unity. Moreover, for exponentially decaying scalar source terms,

$$S_s = S_{o,s} \exp(\beta_s(z - h)), \tag{14a}$$

$$S_T = S_{o,T} \exp(\beta_T(z - h)), \tag{14b}$$

the production term becomes

$$P_d = -\frac{2 \exp(-(z - h)(\beta_Q + \beta_u/l_m))}{a_1 l_m^2 (\beta_u U_o) Q_o} \left( F_s(0) + \frac{S_{o,s}}{\beta_s} \exp(\beta_s(z - h)) \right) \times \left( F_T(0) + \frac{S_{o,T}}{\beta_T} \exp(\beta_T(z - h)) \right).$$

The general solution is  $\overline{T's'} = \overline{T's'_H} + \overline{T's'_p}$ , where  $\overline{T's'_p}$  is a particular solution determined to match this specific production function and the appropriate boundary conditions.

For discussion purposes, three special cases of the normalized production function are considered:

Case 1  $S_{os} = S_{oT} = 0$  and  $F_s(0) \neq 0, F_T(0) \neq 0$ :

Here,  $P_d$  is entirely due to ground sources and sinks and is given by:

$$P_d = -\frac{2F_s(0)F_T(0)}{a_1 l_m^2 (\beta_u U_o) Q_o} \exp((z - h)(-\beta_Q - \beta_u/l_m)).$$

For this set-up,  $P_d$  exponentially increases with increasing  $z/h$  (i.e. becomes less negative with increasing  $z$ ).

Case 2  $F_s(0) = S_{o,T} = 0$ . All other terms are finite:

Here, the production term is due to ground sources for one scalar and foliage sources (or sinks) for the other and is given as:

$$P_d = -\frac{2F_T(0)S_{o,s}}{a_1 l_m^2 (\beta_u U_o) Q_o \beta_s} \exp((z - h)(-\beta_Q - \beta_u/l_m + \beta_s)).$$

Depending on the sign of  $(-\beta_Q - \beta_u/l_m + \beta_s)$ ,  $P_d$  may exponentially increase or decrease with increasing  $z/h$ .

Case 3  $F_s(0) = F_T(0) = 0$ . All other terms are finite:

Here, the production term is entirely due to sources and sinks from the foliage and is given as:

$$P_d = -\left( \frac{2}{a_1 l_m^2 (\beta_u U_o) Q_o} \frac{S_{o,s}}{\beta_s} \frac{S_{o,T}}{\beta_T} \right) \exp((z - h)(-\beta_Q - \beta_u/l_m + \beta_T + \beta_s)).$$

As in case 2,  $P_d$  may exponentially increase or decrease with increasing  $z/h$  depending on the sign of  $(-\beta_Q - \beta_u/l_m + \beta_T + \beta_s)$ .

The canonical form of  $P_d$  in all three cases is given as:

$$P_d(z) = -P_o \exp(\gamma(z - h)),$$

where  $\gamma$  is the attenuation coefficient related to  $\beta_Q, \beta_u/l_m, \beta_T, \beta_s$  depending on whether cases 1, 2, or 3 prevail. For this form of  $P_d(z)$ , the general solution is a superposition of the particular ( $= \overline{T's'_p}$ ) and the homogeneous solutions, leading to

$$\overline{T's'}(z) = \underbrace{\frac{1}{\gamma(\gamma + \beta_Q) - \frac{2}{B_2^2}} [P_d(z)]}_{\overline{T's'_p}} + \underbrace{\left[ \exp\left(-\frac{1}{2}\left(\beta_Q + \frac{B_1}{B_2}\right)z\right) \right] \left[ A_1 + A_2 \exp\left(\frac{B_1}{B_2}z\right) \right]}_{\overline{T's'_H}}, \tag{15}$$

where, as before,  $A_1$  and  $A_2$  are integration constants that must be determined from boundary conditions.

Irrespective of these boundary conditions, the form of the analytical solution above suggests that  $P_d(z)$  (and hence scalar emissions from the soil-canopy system) becomes a dominant term in controlling the vertical variations of  $\overline{T's'}$  when  $|\gamma(\gamma + \beta_Q) - 2/B_2^2| \ll 1$ . Conversely, the precise strength and distribution of the scalar emissions within the soil-canopy system become less relevant when  $|\gamma(\gamma + \beta_Q) - 2/B_2^2| \gg 1$ . When  $|\gamma(\gamma + \beta_Q) - 2/B_2^2| \sim 1$ , both particular and homogeneous solutions significantly contribute to the overall solution. The three special cases earlier described can be thought of as progressive changes in  $\gamma$  (i.e. becoming less and less negative as we proceed from case 1 to case 3). Hence, these three cases are also used to explore different  $|\gamma(\gamma + \beta_Q) - 2/B_2^2|$  regimes (while holding the flow statistics  $\beta_Q$  and  $B_2 = l_m \sqrt{a_1 a_3}$  constant for a given canopy).

### 3.3 Closure Constants ( $a_1$ and $a_3$ )

Since the closure constants should not vary with the presence or absence of vegetation, it is convenient to determine their numerical value in the well-studied ASL rather than the CSL. Hence, to determine  $a_1$  and  $a_3$ , the near-neutral ASL is considered assuming that a balance exists between production and dissipation terms, so that

$$\frac{2}{\lambda_3} Q \overline{T's'} = - \left( \overline{w's' \frac{\partial \overline{T}}{\partial z}} + \overline{w'T' \frac{\partial \overline{s}}{\partial z}} \right). \tag{16}$$

Moreover, for the ASL,  $\partial \overline{T} / \partial z = T_*/(k_v(z - d))$  and  $\partial \overline{s} / \partial z = s_*/(k_v(z - d))$  resulting in

$$\overline{w's' \frac{\partial \overline{T}}{\partial z}} + \overline{w'T' \frac{\partial \overline{s}}{\partial z}} = \frac{2u_*}{k_v(z - d)} (s_* T_*) = \frac{2}{\lambda_3} Q \overline{T's'}. \tag{17}$$

Hence, with  $\lambda_3 = a_3 k_v(z - d)$ ,  $a_3 = \frac{Q \overline{T's'}}{u_* s_* T_*}$ ,  $Q/u_* = \sqrt{A_u^2 + A_v^2 + A_w^2}$ , where  $A_u = \sigma_u/u_* \approx 2.7$ ,  $A_v = \sigma_v/u_* \approx 2.1$ , and  $A_w = \sigma_w/u_* \approx 1.25$ .

Also, in the near-neutral ASL,

$$\frac{\overline{T's'}}{s_* T_*} = R_{Ts} \frac{\sigma_T \sigma_s}{T_* s_*}, \tag{18}$$

where  $R_{Ts}$  is the correlation coefficient between  $T$  and  $s$ . The maximum value of the above quantity occurs when  $R_{Ts} \approx 1$ . Moreover, when using the accepted ASL values for  $\sigma_T/T_* = \sigma_s/s_* \approx A_T = 1.8$  (Sorbjan 1989),  $a_3 = A_T^2 \sqrt{A_u^2 + A_v^2 + A_w^2} \approx 1.8^2 \times 3.65 \approx 11.7$ . The

estimation of  $a_1$  follows from the standard diffusivity analogy, given as  $\lambda_1 Q = a_1 k_v(z - d)$   
 $Q = k_v(z - d)u_*$ , so that  $a_1 = (A_u^2 + A_v^2 + A_w^2)^{-1/2} \approx 0.27$ .

### 4 Results and Discussion

#### 4.1 The Values of $\beta_Q$ and $\beta_T$

In Fig. 1, profiles of measured  $U$ ,  $\sigma_u$ ,  $\sigma_w$ , and  $\overline{u'w'}$  are shown for a number of published CSL experiments, including a uniform dense array of rods in a flume, a rice canopy (that has an approximate constant leaf area density) and a corn canopy, and three forested

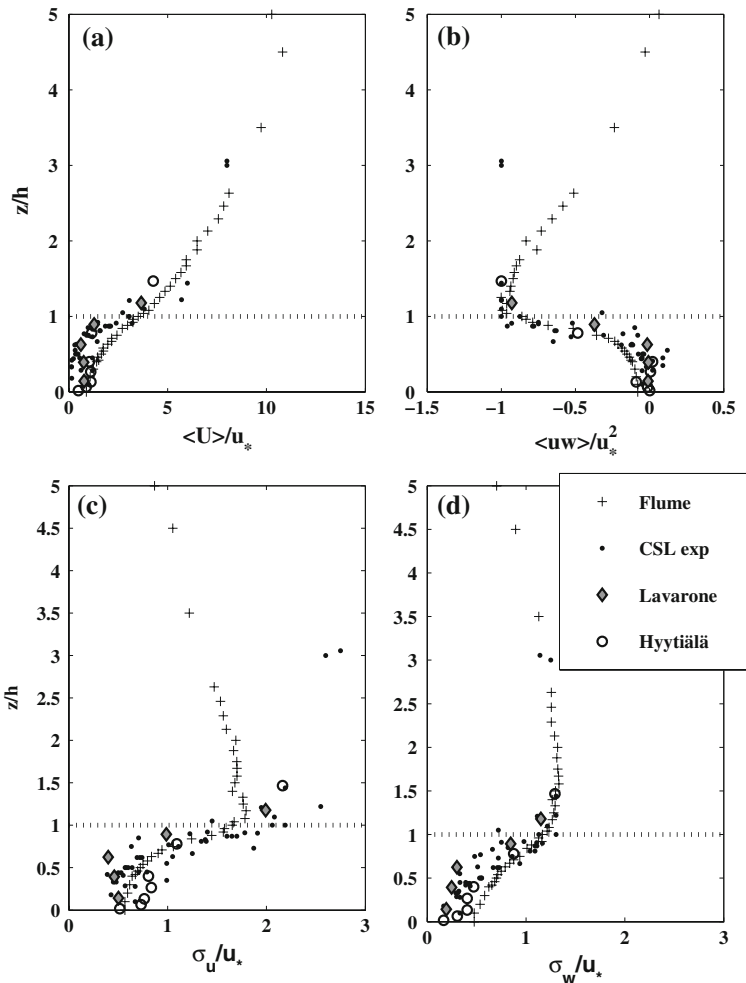


**Fig. 1** Sample of canopy sublayer (CSL) experiments (points: field experiments; crosses: flume experiment) showing profiles of (a) mean velocity  $U$ , (b) Reynolds stress ( $\overline{u'w'}$ ), (c)  $\sigma_u$  and (d)  $\sigma_w$ , across a wide range of canopies described in Katul et al. (2004). The flow statistics collected at the Lavarone Hardwood forest (grey diamonds) and at the Hyttiälä pine forest (circles) are separately shown

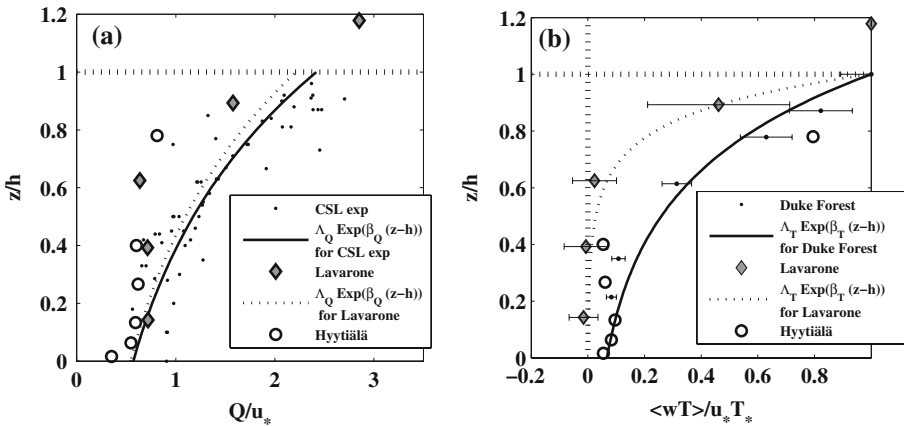


**Fig. 2** The determination of (a)  $\beta_Q$  from the CSL experiments presented in Fig. 1 ( $\beta_Q = 1.44$  for CSL experiments and  $\beta_Q \approx 1.4$  for the Lavarone Hardwood forest and the Hyttiälä pine forest), and (b)  $\beta_T$  for the Duke pine forest (points:  $\beta_T \approx 2.7$ ), for Lavarone Hardwood forest (grey diamonds:  $\beta_T \approx 7$ ) and for Hyttiälä pine forest (circles:  $\beta_T \approx 2.7$ )

ecosystems (spruce, pine, and hardwood canopies with irregular leaf area density distribution). Moreover, two other datasets, one for a dense alpine hardwood canopy in the Lavarone plateau (Italy) and another from a sparser pine forest at Hyttiälä (Finland), are highlighted with separate symbols (Cava et al. 2006; Launiainen et al. 2007). These two experiments are shown separately here because they are employed in model-data comparisons for the two-scalar covariance budgets. For the published CSL experiments,  $Q(z)/u_*$  was computed and regressed with  $z/h$  to yield  $\beta_Q = 1.4$ , shown in Fig. 2a. Using regression analysis,  $\beta_Q \approx 1.4$  was also computed for the Lavarone and the Hyttiälä forest experiments (Fig. 2a). However, for these two experiments, the approximation  $Q = Q_o \exp[\beta_Q(z - h)]$  is not particularly a good choice and a model of the form  $Q = Q_o \exp[\beta_Q(z - h)] + Q'$  is a far superior fit to these two datasets (coefficient of determination  $R^2 > 0.9$ ). Unfortunately, adopting such a model prevents simplified analytical treatment because  $Q^{-1}dQ/dz \neq \beta_Q$  and but is given as

$$\frac{dQ}{Q} = \beta_Q \left( \frac{Q_o \exp[\beta_Q(z - h)]}{Q' + Q_o \exp[\beta_Q(z - h)]} \right).$$

The fact that  $Q^{-1}dQ/dz$  depends on  $z$  prevents an intuitive and simplified analytical treatment.

For the Lavarone and Hyttiälä sites,  $Q'$  is actually comparable to  $Q_o$  suggesting that significant ‘background’ (and inactive) turbulent kinetic energy is maintained without being distorted by the canopy. Hence, when comparing analytical model calculations to measurements, a poorer fit to the  $Q$  data cannot be ignored. For the remaining datasets,  $Q'$  is small and its effect on  $Q^{-1}dQ/dz$  can be absorbed in  $\beta_Q$ .

The availability of multiple sensible heat flux measurements, when expressed as

$$F_{T,n}(z) = \frac{w'T'}{u_* T_*} = F_{T,n}(0) + \Lambda_T \exp(\beta_T(z - h)), \tag{19}$$

permits the estimation of  $\beta_T$ , where  $\Lambda_T$  is the total sensible heat flux emitted by the vegetation only. For illustration, three datasets are considered in Fig. 2b: The Duke pine forest

(in North Carolina, USA) reported in Siqueira et al. (2000), the Lavarone hardwood forest experiment reported in Cava et al. (2006), and the Hyytiälä pine forest experiment (unstable conditions) reported in Launiainen et al. (2007). For the Duke and Hyytiälä datasets shown in Fig. 2  $\beta_T \approx 2.7$ . For the Lavarone hardwood forest,  $\beta_T \approx 7$ , which is almost a factor of 2.5 larger. It is clear that with increasing LAI (3.5–9.6),  $\beta_T$  also increases by roughly the same proportion. At the Lavarone site, much of the sensible heat flux is attenuated in the top 1/3 of the canopy while the remaining sensible heat flux is almost negligible for the remaining 2/3 of the canopy depth. For both pine forest experiments, the sensible heat flux remains finite even at the forest floor.

The implications of finite versus negligible ground heat fluxes and emissions by the canopy are explored using hypothetical cases (1–3). Model calculations for these hypothetical scenarios form a logical basis to compare against field experiments. Following the discussion of the hypothetical cases, comparisons with the Hyytiälä data (ensemble profiles) and the Lavarone data (one level inside the canopy but varying  $\overline{T'q'}$  at  $z/h = 1$  every 30 min) are presented.

### 4.2 Model Results

The covariance budget between temperature and water vapour within the canopy is considered for model illustration. To avoid the difficulty in specifying a Dirichlet-type (or state-dependent) boundary condition at the ground for  $\overline{T'q'}$ , a Neumann type (or flux-dependent) boundary condition is selected instead. Hence, the boundary conditions imposed on all the model runs throughout are  $\overline{T'q'(h)}/T_*q_* = (A_T)^2$  at  $z/h = 1$  (i.e. the maximum value anticipated from ASL similarity theory) and  $d\overline{T'q'}/dz = 0$  at  $z/h = 0$ . The canopy parameters selected here are  $C_d = 0.2$  (typical for terrestrial vegetation),  $h = 20$  m (typical of a maturing forest),  $LAI = 5 \text{ m}^2 \text{ m}^{-2}$  (typical of a closed and dense forest canopy),  $\beta_u = 1/3$  (typical for dense vegetation), and  $\beta_Q = 1.44$ . Table 1 shows sample values for sensible and latent heat fluxes used in cases 1–3. Scalar fluxes are displayed throughout in equivalent energy fluxes of heat and water vapour so that scalar source units can be readily compared.

For case 1 (i.e. both scalars emitted from the ground),  $P_d$  exponentially increases with increasing  $z/h$  (i.e. becomes less negative) with no modifications from the scalar source attenuation coefficients. For this case,  $\gamma = -\beta_Q - \beta_u/l_m$  and  $B_2^2 \approx 3.16 l_m^2$ , resulting in  $B_2^2 \gamma (\gamma + \beta_Q) \approx 0.3 + \left(\frac{0.1}{C_d}\right) \frac{h}{LAI} \approx 2.3$ , which suggests that  $|B_2^2 \gamma (\gamma + \beta_Q) - 2| = 0.3$

**Table 1** Sample cases illustrating how various combinations of ground fluxes and scalar source attenuation profiles affect  $P_d$  and  $\overline{T'q'(z)}$  as discussed in Sect. 3.2

Case	$q$			$T$		
	$F_q(0)$	$S_{o,q}$	$\beta_c$	$F_T(0)$	$S_{o,T}$	$\beta_T$
1	100	0	–	100	0	–
2	0	200	0.70	100	0	–
3	0	200	0.70	0	200	0.70
4	0	20	0.07	–100	200	0.70

Here  $F_s(0)$  is the forest floor flux of scalar  $s$  (either water vapour  $q$  or air temperature  $T$ ),  $S_{o,s}$  is the foliage source or sink of  $s$ , and  $\beta_s$  is the attenuation coefficient of the scalar flux. All calculations are carried out assuming  $u_* = 0.3 \text{ m s}^{-1}$ ,  $A_u = 2.7$ ,  $A_v = 2.1$ , and  $A_w = 1.25$ ,  $\beta_u = 1/3$ ,  $\beta_Q = 1.44$ ,  $LAI = 5 \text{ m}^2 \text{ m}^{-2}$ ,  $h = 20$  m, and  $C_d = 0.2$ . Units are  $\text{W m}^{-2}$  for sensible and latent heat fluxes

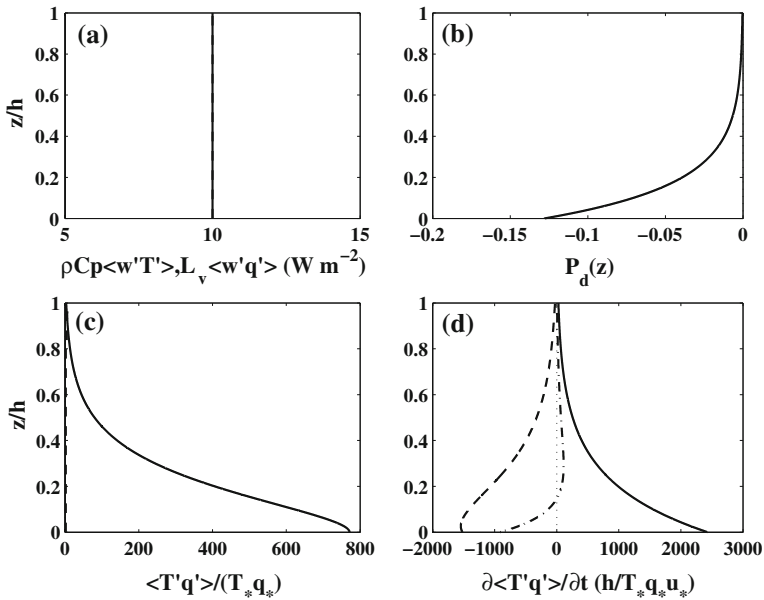


**Fig. 3** Model calculations for case 1: (a) The assumed latent ( $L_v \overline{w'q'}$ ) and sensible ( $\rho C_p \overline{w'T'}$ ) heat flux profiles; (b) the modelled normalized production term ( $P_d$ ) profile (Eq. 6); (c) the modelled  $\overline{T'q'}$  profiles using the full solution (solid) and the homogeneous solution (dashed), and (d) the modelled profiles of the three components of the budget equation  $\partial \overline{T'q'}/\partial t = 0$  (Eqs. 1–3) with production in solid, dissipation in dashed, and flux-transport in dot-dashed. All velocity and length scale variables are normalized by  $u_*$  and canopy height  $h$ , respectively, while all scalars are normalized by their respective surface-layer values ( $T_*$  or  $q_*$ ) at the canopy top

is rather small ( $\ll 1$ ), and  $\overline{T'q'}$  ought to be controlled by the particular solution (i.e.  $P_d$ ) with the homogeneous solution playing a negligible role. Figure 3 shows that  $\overline{T'q'}$  is, indeed, governed by  $P_d$  and the homogeneous solution does not contribute to the overall solution. In fact,  $\overline{T's'(0)} \gg \overline{T's'(h)}$  for this configuration. It should be emphasized here that the flux-transport term (Eqs. 1–3) plays a significant ‘dissipative’ role in balancing the production term near the ground (see Fig. 3).

For case 2, when one scalar is emitted at the ground while the other scalar is emitted from the foliage,  $P_d$  becomes less negative near the ground, but  $|B_2^2 \gamma (\gamma + \beta_Q) - 2|$  is no longer small. Hence, the homogeneous solution here becomes a significant contributor to the overall solution. Figure 4 shows that the homogeneous solution and the full solution both decay with decreasing  $z/h$  (Fig. 4); however, the attenuation of the full solution is slower due to the contribution of the scalar source, as expected.

For case 3, when both scalar sources are emitted from the foliage with no ground emissions,  $P_d$  still exponentially decreases (i.e. becomes less negative) with increasing  $z/h$ , but  $|B_2^2 \gamma (\gamma + \beta_Q)|$  is now much larger than 2. The overall solution is primarily governed by the homogeneous solution, which decays rapidly inside the canopy. Figure 5 shows that the effective attenuation of both solutions is comparable. Note that, near the canopy top, the dissipation is larger than the production (opposite to case 1 at  $z/h = 0$ ), and the flux-transport balances this ‘excess’ dissipation.

As further analysis, we consider a case 4 where one scalar is absorbed at the ground and emitted by the canopy while another scalar is emitted by the canopy but with a small

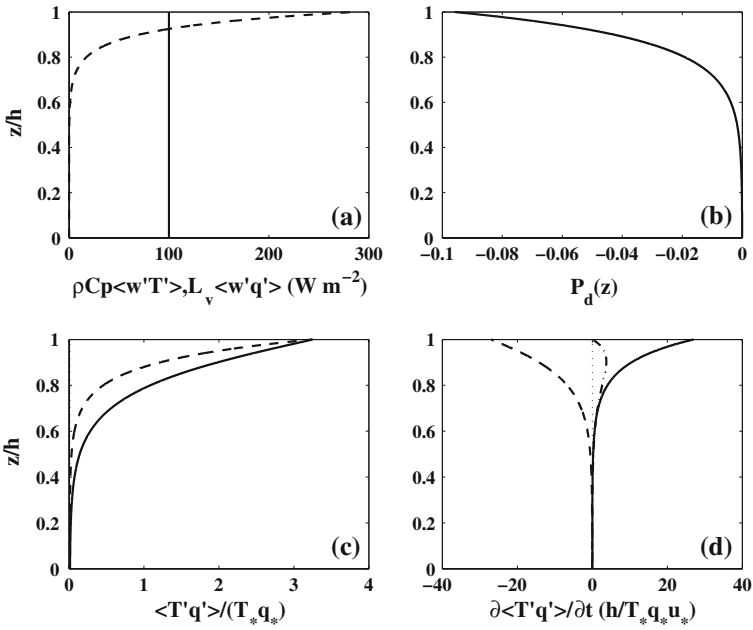


Fig. 4 Same as Fig. 3 but for case 2

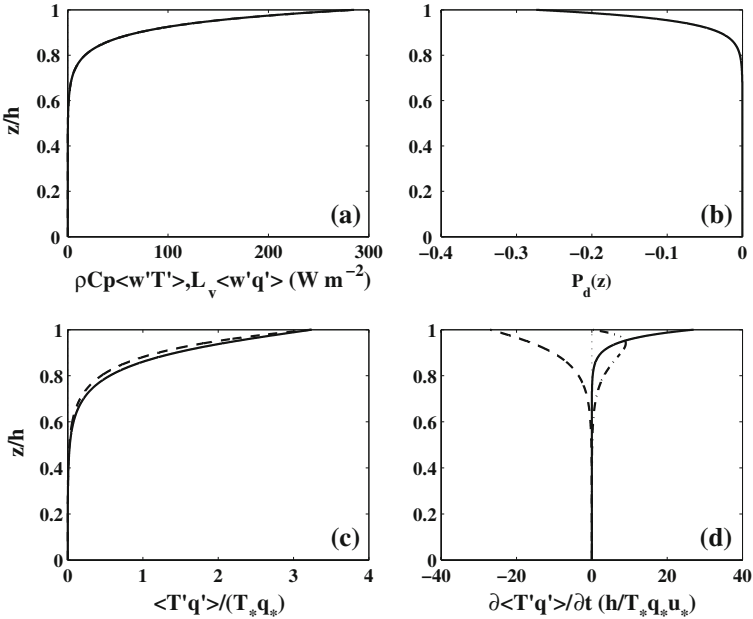


Fig. 5 Same as Fig. 3 but for case 3

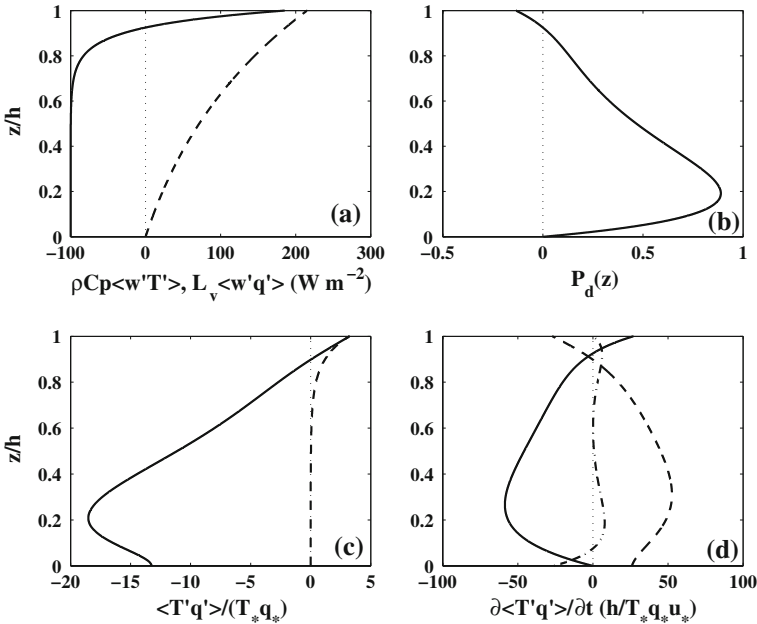
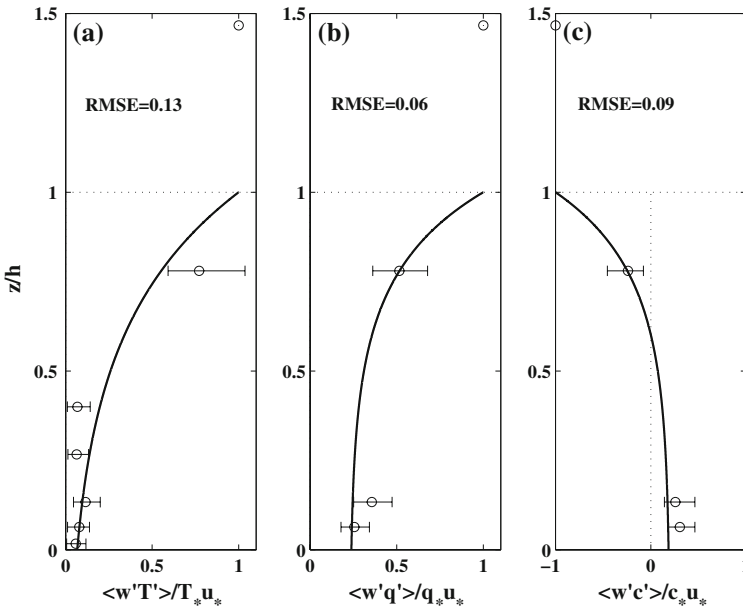


Fig. 6 Same as Fig. 3 but for case 4

attenuation coefficient as shown in Fig. 6 (quasi-linear decline with decreasing  $z/h$ ). In this case,  $P_d$  is a combination of all three previous cases and becomes non-monotonic. The solution for  $\overline{T's'}$ , graphically shown in Fig. 6 (but not explicitly listed here), can switch sign within the canopy volume. For these cases, the departure between the homogeneous and particular solutions is significantly large, and the scalar source emissions do play a major role in the vertical variations of  $\overline{T's'}$ .

### 4.3 Comparison with the Hyytiälä Experiment

To assess whether the proposed model describes the main attributes of the  $\overline{T's'}$  variation in forested ecosystems, qualitative comparisons with measurements reported from the Hyytiälä Scots pine site (SMEAR II) are discussed next. The experimental set-up and data processing are all described elsewhere (Launiainen et al. 2007) and are not repeated here. We should note that the Hyytiälä forest experiment is far from ‘ideal’ for precise model validation because: (1) much of the  $LAI (= 3.5 \text{ m}^2 \text{ m}^{-2})$  is clustered in the top part of the canopy thereby making the leaf area density far from uniform, (2) an approximate linear mixing length in the bottom 20% of the canopy was reported elsewhere (Launiainen et al. 2007), again suggestive that the constant mixing length assumption cannot be entirely accurate for this set-up (especially near the forest floor), and (3) the mean velocity profile and  $Q$  are not well described by an exponential model (evident in Fig. 1). Despite the departure between the model assumptions and the site characteristics here, these data are used because of the availability of (1) detailed flux profiles for all three scalars ( $c$ ,  $q$ , and  $T$ ) where  $c$  is the  $\text{CO}_2$  concentration, (2) two-scalar covariances for all three scalar combinations ( $\overline{c'T'}$ ,  $\overline{c'q'}$ , and  $\overline{T'q'}$ ), and (3) triple moments for all three scalar combinations ( $\overline{w'T'c'}$ ,  $\overline{w'q'T'}$ , and  $\overline{w'c'q'}$ ). Here, unstable atmospheric stability conditions, as defined in Launiainen et al. (2007), are considered to ensure reliable measured fluxes above the canopy and sufficiently large (in magnitude) triple moments.



**Fig. 7** Comparison between measured (open circles) and assumed vertical attenuation of (a)  $\overline{w'T'}/(u_*T_*)$ , (b)  $\overline{w'q'}/(u_*q_*)$ , and (c) the CO<sub>2</sub> flux  $\overline{w'c'}/u_*c_*$ , by the canopy. Symbols represent the medians and the horizontal bars represent the uncertainty (median 25th–median 75th). The height from the forest floor ( $z$ ) is normalized by the canopy height ( $h$ ). The  $q$  and  $c$  concentrations at the lowest two levels were corrected for density fluctuations (see [Detto and Katul 2007](#)) because they were sampled using an open-path gas analyzer. All other scalar concentration measurements were sampled with closed-path gas analyzers. The root-mean square error (RMSE) between observed and modelled values is shown for each panel

Figures 1 and 2 have already presented the profiles of  $U/u_*$  and  $Q/u_*$  for the Hyttiälä forest. Using regression analysis on these data, it was already shown that  $\beta_Q = 1.44$  when  $Q = Q_o \exp[\beta_Q(z - h)]$  though this value must be treated with some care given the indirect influence of  $Q'$  (in  $Q = Q_o \exp[\beta_Q(z - h)] + Q'$ ). When repeating the same analysis for the mean velocity, the resulting  $\beta_u = u_*/U = 0.25$  and is less than the expected 0.33 for dense canopies consistent with the fact that  $\beta_u$  is usually lower for a sparser canopy ([Massman 1997](#); [Poggi et al. 2004](#)). When expressing  $l_m = 2\beta_u^3 h / (C_d LAI)$ ,  $C_d = 0.1$  was determined by matching the Reynolds stress profile for  $LAI = 3.5 \text{ m}^2 \text{ m}^{-2}$  and  $h = 15 \text{ m}$ . Also, using the data in Fig. 1,  $A_u = 2.16$ ,  $A_w = 1.3$ , and  $A_v = 2.05$  taken from elsewhere ([Launiainen et al. 2007](#)) result in  $Q_o = 3.25$  (see Fig. 2), a value close to the standard ASL value. For near-neutral conditions, the data in [Launiainen et al. \(2007\)](#) also suggest that  $A_T = 1.4$  (used here), which is less than the 1.8 earlier assumed for ASL flows. When all these constants are taken together,  $a_1 = 0.3$ ,  $a_3 = 6.36$ , and  $B_2 = \sqrt{a_1 a_3 l_m^2} = 2.18$ , resulting in  $B_1 = \sqrt{8 + (\beta_Q B_2)^2} = 4.23$ .

Figure 7 shows the measured attenuation profile of the scalar fluxes and the exponential fit to them. For heat  $\beta_T = 2.7$  consistent with the Duke Forest pine experiment as earlier noted (repeated for convenience here), but for water vapour and CO<sub>2</sub>,  $\beta_c = \beta_q = 4.5$ , much higher than for heat. In a first-order analysis,  $\gamma = -\beta_Q - \beta_u/l_m + \beta_T + \beta_s \approx 5.6$  resulting in  $|B_2^2 \gamma (\gamma + \beta_Q)| \gg 2$ . Hence, far from the ground sources and sinks (i.e. analogous to case 3), we expect that the homogeneous solution explains the vertical variation

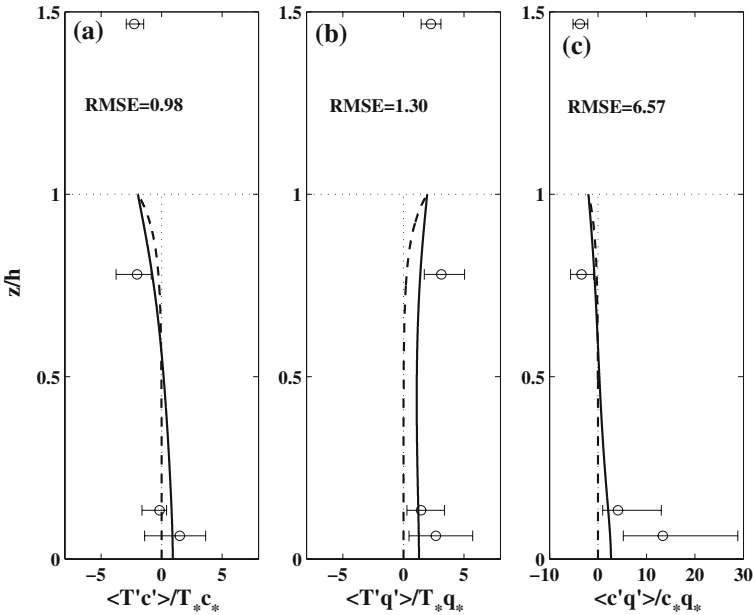


**Fig. 8** Comparison between measured (open circles) and modelled (lines) vertical variation of (a)  $\overline{T'c'}/(T_*c_*)$ , (b)  $\overline{T'q'}/(T_*q_*)$ , and (c) the CO<sub>2</sub> flux  $\overline{q'c'}/(q_*c_*)$ , by the canopy. Symbols and horizontal bars are as in Fig. 7. The height from the forest floor ( $z$ ) is normalized by the canopy height ( $h$ ). Dashed lines are for the homogeneous solution ( $P_d = 0$ ) and solid lines are for the full solution. The  $q$  and  $c$  concentrations at the lowest two levels were corrected for density fluctuations (see Detto and Katul 2007) because they were sampled using an open-path gas analyzer. All other scalar concentration measurements were sampled with closed-path gas analyzers

of the two-scalar covariances. Near the ground, however, the situation reverses and case 1 becomes prevalent, where  $P_d$  becomes the dominant term (all three scalars have finite ground sources as shown from Fig. 7). Figure 8 compares the measured and modelled profiles of the two-scalar covariances  $\overline{c'T'}$ ,  $\overline{c'q'}$ , and  $\overline{T'q'}$ , using the homogeneous and non-homogeneous model solutions. For all three two-scalar covariance budgets, the homogeneous solution is a significant contributor to the two-scalar covariances near the canopy top. However, near the forest floor, the ground fluxes (via  $P_d$ ) affect the two-scalar covariances. Figure 9 presents the comparison between measured and modelled (i.e. Eq. 3) triple moments for all three scalars. The agreement between measured and modelled triple moments is surprisingly good given all the assumptions made in the derivation and the less than optimum agreement reported in Fig. 8.

#### 4.4 Comparison with the Lavarone Experiment

While the Hyttiälä experiment discussed model results in terms of ensemble profiles, the Lavarone experiment is intended to compare how well the model describes variations in  $\overline{T's'}$  deep inside the canopy from observed variations in  $\overline{T's'}$  above the canopy. The experimental set-up and data processing are described elsewhere (Cava et al. 2006, 2008; Cava and Katul 2008) and are not repeated here. We only note that five sonic anemometers (four inside the canopy and one above) and two gas analyzers (one above and one near the forest floor)

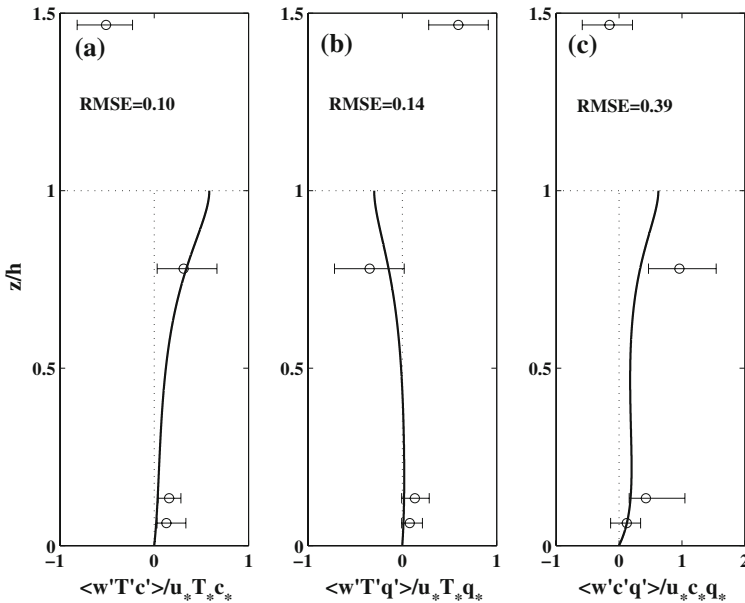


**Fig. 9** Comparison between measured (open circles) and modelled (solid line) vertical attenuation of (a)  $\overline{w'T'c'}/(u_*T_*c_*)$ , (b)  $\overline{w'T'q'}/(u_*T_*q_*)$ , and (c) the CO<sub>2</sub> flux  $\overline{w'q'c'}/(u_*q_*c_*)$ , by the canopy. Symbols and horizontal bars are as in Fig. 7. The height from the forest floor ( $z$ ) is normalized by the canopy height ( $h$ ). The  $q$  and  $c$  concentrations at the lowest two levels were corrected for density fluctuations (see Detto and Katul 2007) because they were sampled using an open-path gas analyzer. All other scalar concentration measurements were sampled with closed-path gas analyzers

were used in this set-up. The analysis was performed on 11 days during daytime conditions (between 0900 and 1500 local time) resulting in about 140 30-min runs; runs exhibiting clear non-stationarity were discarded. All the velocity parameters  $\beta_u$ ,  $\beta_Q$ ,  $I_m$ ,  $Q_o$ ,  $A_u$ ,  $A_v$ , and  $A_w$  were determined from the regression on ensemble data shown in Figs. 1 and 2. From the regression analysis on the mean velocity profile,  $\beta_u = u_*/\bar{U} = 0.2$ , which is less than the expected value for dense canopies ( $= 0.33$ ). We should note here that the exponential model does not describe well the mean velocity profile for the Lavarone experiment due to the clustering of leaves near the canopy top. Hence, no physical significance is attached to this value of  $\beta_u$ . The regression analysis yielded  $\beta_Q \approx 1.4$  though this value should be treated with caution given the contributions from  $Q'$ . The  $A_u = 2.0$ ,  $A_v = 1.7$ ,  $A_w = 1.2$  (i.e.  $Q_o = 2.9$ ), and  $A_T = 2.3$  were all taken from Cava et al. (2008). Five levels of sensible heat flux measurements were used to determine  $F_T(0)$ ,  $S_{o,T}$ ,  $\beta_T$  every 30 min. For water vapour, only two flux measurement levels were available necessitating additional simplifications to describe the water vapour flux profile. Given that the Lavarone site is dry in the summer,  $F_q(0) \approx 0$ , and the two eddy-covariance water vapour flux measurements were used to infer  $S_{o,q}$ ,  $\beta_q$  every 30 min but with no redundancy (i.e. the number of parameters to be determined is identical to the number of measurements and hence the lack of statistical robustness in the parameter estimation). Using measured  $\overline{T'q'}$  and  $u_*$  above the canopy every 30 min as boundary conditions, the model calculated  $\overline{T'q'}$  at  $z/h = 0.14$  and compared it with the measured value. Figure 10 shows the comparison between measured and computed  $\overline{T'q'}/(T_*q_*)$  for both the homogeneous solution and the full solution; each point refers to the

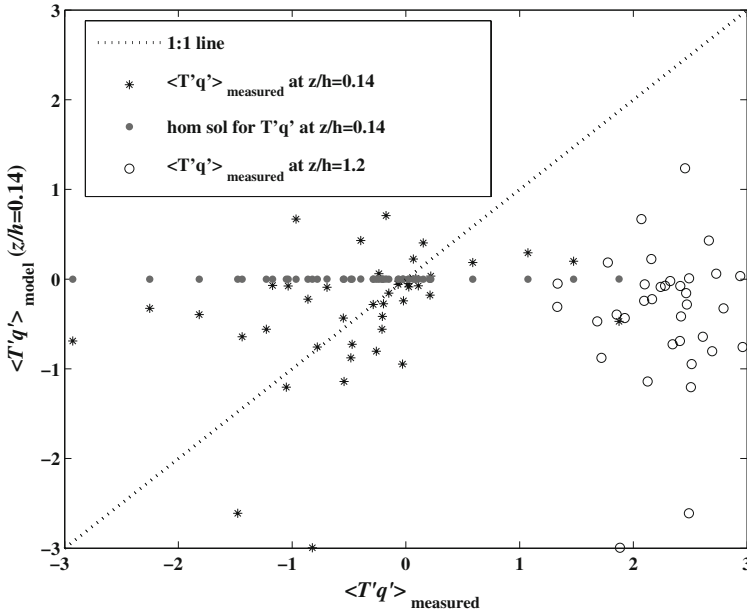


**Fig. 10** Comparison between measured (Hardwood forest, Lavarone, Italy) and modelled  $\overline{T'q'}/(T_*q_*)$  at  $z/h = 0.14$  for both the homogeneous (grey points) and full solution (black stars). For reference, the comparison between measured  $\overline{T'q'}/(T_*q_*)$  above the canopy top (i.e. the model input) and the modelled values at  $z/h = 0.14$  is also shown (circles). Each point refers to the ensemble mean value obtained by dividing the range of  $\overline{T'q'}/(T_*q_*)$  variation in interval of 0.05. Dashed line refers to 1:1 line. All  $q$  and  $c$  concentrations were corrected for density fluctuations (see [Detto and Katul 2007](#)) because they were sampled using an open-path gas analyzer

ensemble mean values obtained by dividing the range of  $\overline{T'q'}/(T_*q_*)$  variation in intervals of 0.05. Ensemble means were computed for each interval for two reasons: (1) to obtain robust statistics in model/data comparisons given the lack of redundancy in  $S_{o,q}$ ,  $\beta_q$ , and (2) to represent the combined space-time averages required by the model via ensemble averages. The comparison between measured  $\overline{T'q'}/(T_*q_*)$  above the canopy top at  $z/h = 1.2$  (i.e. the model input) and the modelled values at  $z/h = 0.14$  are also shown for reference. From Fig. 10, the following can be noted:

- (1) the correlation between  $\overline{T'q'}/(T_*q_*)$  at the canopy top and  $\overline{T'q'}/(T_*q_*)$  at  $z/h = 0.14$  is weak;
- (2) the homogeneous solution provides no information about  $\overline{T'q'}/(T_*q_*)$  at  $z/h = 0.14$  from  $\overline{T'q'}/(T_*q_*)$  measured at the canopy top (correlation coefficient  $R \approx 0$ ). This result suggests that  $\overline{T'q'}/(T_*q_*)$  at the bottom of the canopy is primarily controlled by scalar source-sink emissions at the ground consistent with earlier arguments;
- (3) the full analytical solution appears to correctly transfer the  $\overline{T'q'}/(T_*q_*)$  measured at the canopy top to  $\overline{T'q'}/(T_*q_*)$  at  $z/h = 0.14$  (i.e. data points are clustered around the 1:1 line and  $R \approx 0.35$ ). By transfer here, we mean that the analytical solution provides new information about the variability in  $\overline{T'q'}/(T_*q_*)$  at  $z/h = 0.14$  beyond the variability forced by the boundary condition at  $z/h = 1$ . However, the scatter remains large in the 30-min data-model comparisons. The reason this scatter is not surprising is attributed to the large uncertainty in the 30-min measurements, the uncertainty in the eddy

diffusivity used in the model, and the uncertainty in the turbulent kinetic energy attenuation profile. Cava and Katul (2008) already showed that the length scale responsible for vertical transport in the trunk space of this stand is consistent with vortex shedding from stems and this length scale is not reflected in  $l_m$ . Notwithstanding all these criticisms, the analytical model ‘injects’ new information about the variability in  $\overline{T'q'}/(T_*q_*)$  near the ground beyond that provided by the upper boundary condition.

## 5 Conclusions

The budget equation for the two-scalar covariance (e.g.  $\overline{T's'}$ ) in a stationary and planar homogeneous high Reynolds number flow, in the absence of subsidence, was considered within the canopy sublayer. When standard closure approximations for the transport and dissipation terms were employed, along with first-order closure principles for a component of the production term, a second-order ordinary differential equation (ODE) describing the vertical variations in  $\overline{T's'}$  was derived. For an exponentially varying turbulent kinetic energy, and for a constant mixing length, the homogeneous solution of this ODE can be solved analytically. The homogeneous solution describes how a finite  $\overline{T's'}$  at the canopy top is transported and dissipated within the canopy volume. The attenuation rate of a specified  $\overline{T's'}$  at  $z/h = 1$ , in the absence of local sources and sinks, was shown to be governed by  $L_c = (C_d a)^{-1}$  (the adjustment length scale),  $\beta_u = u_*/U$  (the mean momentum absorption coefficient at the canopy top), and  $\beta_Q$  (linked to the turbulent kinetic energy attenuation coefficient within the canopy). When modelling the mean scalar concentration gradients arising in the local production terms using first-order closure principles, and assuming that the scalar source emissions decay exponentially within the canopy, a general solution describing the vertical variation of  $\overline{T's'}$  was presented. Within this model framework, it was demonstrated that:

- (1) Two regimes emerge—one in which the vertical variation in  $\overline{T's'}$  is primarily dictated by  $L_c$ ,  $\beta_u$ , and  $\beta_Q$  and given by the homogeneous solution (reflecting contributions from transport and dissipation terms), and a second that is strongly sensitive to the scalar source-sink emission parameters (due to the local production term). It was shown that this first regime dominates the  $\overline{T's'}$  solution when  $|\gamma(\gamma + \beta_Q) - 2/B_2^2| \gg 1$ , where  $B_2 = l_m \sqrt{a_1 a_3}$ ,  $l_m = 2\beta_u^3 L_c$ ,  $\gamma = (-\beta_Q - \beta_u/l_m + \beta_T + \beta_s)$ ,  $\beta_T$  and  $\beta_s$  are the scalar source (or sink) attenuation coefficients, and  $a_1$  and  $a_3$  are closure coefficients that can be determined from atmospheric surface-layer (ASL) similarity theory.
- (2) The vertical variations in  $\overline{T's'}$  need not be monotonic even when the two-scalar source distributions monotonically decay inside the canopy.
- (3) Despite the restrictive assumptions of the analytical model, the model captures the key patterns of the observed  $\overline{T's'}$  in two very distinct forested ecosystems.

There are a number of generalizations that can be implemented within this model framework—for example, revising the production term to avoid the use of  $K$  theory, accounting for the non-constant  $dQ/Q$ , linking the source parameters (e.g.  $\beta_s$ ) to physiological, radiative, and canopy aerodynamic parameters, and matching this CSL solution to a recently proposed ASL solution (Katul et al. 2008) so that modulations from the outer layer can be propagated down inside the canopy. This latter mechanism was shown to be important for scalar variances inside the canopy (Cava et al. 2008). These revisions, while they do not affect the homogeneous solution, permit direct calculations of how scalar source/sink dissimilarity within the canopy affect  $\overline{T's'}$  and concomitant processes, such as that represented by the buoyancy term in the scalar flux budget equation or segregation ratios for certain chemically reactive species.

Hence, the results here do not provide ‘finality’ to the problem of modelling the two-scalar covariance inside the canopy. Rather, they are intended to initiate discussions on the role of canopy processes, whether it be attenuation of the flow statistics or emission patterns in scalar sources and sinks on  $\overline{T's'}$ . Moreover, the framework adopted here can benefit from high-resolution large-eddy simulation experiments that explore optimum closure schemes for the flux-transport and dissipative terms in the two-scalar covariance budgets both in the CSL and ASL.

**Acknowledgements** G. Katul acknowledges support from the National Science Foundation (NSF-EAR 06-35787, NSF-EAR-06-28432, and NSF-ATM-0724088), the Binational Agricultural Research and Development (BARD, Research Grant No. IS3861-06), and the US Department of Energy (DOE) through the office of Biological and Environmental Research (BER) Terrestrial Carbon Processes (TCP) program (Grants # 10509-0152, DE-FG02-00ER53015, and DE-FG02-95ER62083). D. Cava acknowledges support from ‘Cooperazione Italia-USA su Scienza e Tecnologia dei Cambiamenti Climatici, Anno 2006-2008’. S. Launiainen and T. Vesala acknowledge EU-funded projects CarboEurope, IMECC and ICOS and Academy of Finland.

## References

- Asanuma J, Tamagawa I, Ishikawa H, Ma YM, Hayashi T, Qi YQ, Wang J (2007) Spectral similarity between scalars at very low frequencies in the unstable atmospheric surface layer over the Tibetan plateau. *Boundary-Layer Meteorol* 122(1):85–103. doi:[10.1007/s10546-006-9096-y](https://doi.org/10.1007/s10546-006-9096-y)
- Cava D, Katul GG (2008) Spectral short-circuiting and wake production within the canopy trunk space of an alpine hardwood forest. *Boundary-Layer Meteorol* 126(3):415–431. doi:[10.1007/s10546-007-9246-x](https://doi.org/10.1007/s10546-007-9246-x)
- Cava D, Katul GG, Scrimieri A, Poggi D, Cescatti A, Giostra U (2006) Buoyancy and the sensible heat flux budget within dense canopies. *Boundary-Layer Meteorol* 118(1):217–240. doi:[10.1007/s10546-005-4736-1](https://doi.org/10.1007/s10546-005-4736-1)
- Cava D, Katul GG, Sempreviva AM, Giostra U, Scrimieri A (2008) On the anomalous behavior of scalar flux-variance similarity functions within the canopy sub-layer of a dense Alpine forest. *Boundary-Layer Meteorol* 128:33–57. doi:[10.1007/s10546-008-9276-z](https://doi.org/10.1007/s10546-008-9276-z)
- Cionco RM (1965) A mathematical model for air flow in a vegetative canopy. *J Appl Meteorol* 4:517–522. doi:[10.1175/1520-0450\(1965\)004<0517:AMMFAF>2.0.CO;2](https://doi.org/10.1175/1520-0450(1965)004<0517:AMMFAF>2.0.CO;2)
- Coulman CE (1980) Correlation between velocity, temperature and humidity fluctuations in the air above land and ocean. *Boundary-Layer Meteorol* 19:403–420. doi:[10.1007/BF00122342](https://doi.org/10.1007/BF00122342)
- Detto M, Katul GG (2007) Simplified expressions for adjusting higher-order turbulent statistics obtained from open path gas analyzers. *Boundary-Layer Meteorol* 122(1):205–216. doi:[10.1007/s10546-006-9105-1](https://doi.org/10.1007/s10546-006-9105-1)
- Finnigan JJ, Belcher SE (2004) Flow over a hill covered with a plant canopy. *Q J Roy Meteorol Soc* 130:1–29. doi:[10.1256/qj.02.177](https://doi.org/10.1256/qj.02.177)
- Friehe C, LaRue J, Champagne F, Gibson C, Dreyer GF (1975) Effects of temperature and humidity fluctuations on the optical refractive index in the marine boundary layer. *J Opt Soc Am* 65:1502–1511. doi:[10.1364/JOSA.65.001502](https://doi.org/10.1364/JOSA.65.001502)
- Gao W, Wesely ML (1994) Numerical modeling of the turbulent fluxes of chemically reactive trace gases in the atmospheric boundary-layer. *J Appl Meteorol* 33:835–847. doi:[10.1175/1520-0450\(1994\)033<0835:NMOTTF>2.0.CO;2](https://doi.org/10.1175/1520-0450(1994)033<0835:NMOTTF>2.0.CO;2)
- Gao W, Wesely ML, Doskey PV (1993) Numerical modeling of the turbulent-diffusion and chemistry of  $\text{NO}_x$ ,  $\text{O}_3$ , Isoprene, and other reactive trace gases in and above a forest canopy. *J Geophys Res Atmos* 98:18339–18353
- Garratt JR (1992) *The atmospheric boundary layer*. Cambridge University Press, Cambridge, 316 pp
- Inoue E (1963) On the turbulent structure of airflow within crop canopies. *J Meteorol Soc Jpn* 41:317–326
- Juang JY, Katul GG, Siqueira MB, Stoy PC, Palmroth S, McCarthy HR, Kim HS, Oren R (2006) Modeling nighttime ecosystem respiration from measured  $\text{CO}_2$  concentration and air temperature profiles using inverse methods. *J Geophys Res Atmos* 111(D8):D08s05
- Juang JY, Katul GG, Siqueira MB, Stoy PC, McCarthy HR (2008) Investigating a hierarchy of Eulerian closure models for scalar transfer inside forested canopies. *Boundary-Layer Meteorol* 128:1–32. doi:[10.1007/s10546-008-9273-2](https://doi.org/10.1007/s10546-008-9273-2)
- Katul GG, Mahrt L, Poggi D, Sanz C (2004) One and two equation models for canopy turbulence. *Boundary-Layer Meteorol* 113:81–109. doi:[10.1023/B:BOUN.0000037333.48760.e5](https://doi.org/10.1023/B:BOUN.0000037333.48760.e5)

- Katul GG, Finnigan JJ, Poggi D, Leuning R, Belcher S (2006) The influence of hilly terrain on canopy-atmosphere carbon dioxide exchange. *Boundary-Layer Meteorol* 118:189–216. doi:[10.1007/s10546-005-6436-2](https://doi.org/10.1007/s10546-005-6436-2)
- Katul GG, Sempreviva AM, Cava D (2008) The temperature-humidity covariance in the marine surface layer: a one-dimensional analytical model. *Boundary-Layer Meteorol* 126:263–278. doi:[10.1007/s10546-007-9236-z](https://doi.org/10.1007/s10546-007-9236-z)
- Lamaud E, Irvine M (2006) Temperature-humidity dissimilarity and heat-to-water-vapor transport efficiency above and within a pine forest canopy: the role of the Bowen ratio. *Boundary-Layer Meteorol* 120(1):87–109. doi:[10.1007/s10546-005-9032-6](https://doi.org/10.1007/s10546-005-9032-6)
- Launiainen S, Vesala T, Mölder M, Mammarella I, Smolander S, Rannik Ü et al (2007) Vertical variability and effect of stability on turbulence characteristics down to the floor of a pine forest. *Tellus* 59B:919–936. doi:[10.1111/j.1600-0889.2007.00313.x](https://doi.org/10.1111/j.1600-0889.2007.00313.x)
- Massman WJ (1997) An analytical one-dimensional model of momentum transfer by vegetation of arbitrary structure. *Boundary-Layer Meteorol* 83(3):407–421. doi:[10.1023/A:1000234813011](https://doi.org/10.1023/A:1000234813011)
- Massman WJ, Weil JC (1999) An analytical one-dimensional second-order closure model of turbulence statistics and the Lagrangian time scale within and above plant canopies of arbitrary structure. *Boundary-Layer Meteorol* 91:81–107. doi:[10.1023/A:1001810204560](https://doi.org/10.1023/A:1001810204560)
- Meyers TP, Paw UKT (1987) Modeling the plant canopy micrometeorology with higher-order closure principles. *Agric Meteorol* 41(1–2):143–163. doi:[10.1016/0168-1923\(87\)90075-X](https://doi.org/10.1016/0168-1923(87)90075-X)
- Moriwaki R, Kanda M (2006) Local and global similarity in turbulent transfer of heat, water vapor, and CO<sub>2</sub> in the dynamic convective sublayer over a suburban area. *Boundary-Layer Meteorol* 120(1):163–179. doi:[10.1007/s10546-005-9034-4](https://doi.org/10.1007/s10546-005-9034-4)
- Patton EG, Davis K, Barth MC, Sullivan PP (2001) Decaying scalars emitted by a forest canopy: a numerical study. *Boundary-Layer Meteorol* 100:91–129. doi:[10.1023/A:1019223515444](https://doi.org/10.1023/A:1019223515444)
- Poggi D, Porporato A, Ridolfi L, Albertson JD, Katul GG (2004) The effect of vegetation density on canopy sub-layer turbulence. *Boundary-Layer Meteorol* 111(3):565–587. doi:[10.1023/B:BOUN.0000016576.05621.73](https://doi.org/10.1023/B:BOUN.0000016576.05621.73)
- Raupach MR, Shaw RH (1982) Averaging procedures for flow within vegetation canopies. *Boundary-Layer Meteorol* 22:79–90. doi:[10.1007/BF00128057](https://doi.org/10.1007/BF00128057)
- Roth M, Oke TR (1995) Relative efficiencies of turbulent transfer of heat, mass, and momentum over a patchy urban surface. *J Atmos Sci* 52(11):1863–1874. doi:[10.1175/1520-0469\(1995\)052<1863:REOTTO>2.0.CO;2](https://doi.org/10.1175/1520-0469(1995)052<1863:REOTTO>2.0.CO;2)
- Saito T (1964) On the wind profile within plant communities. *Bull Nat Inst Agric Sci Jpn* 11:67–73
- Sempreviva AM, Hojstrup J (1998) Transport of temperature and humidity variance and covariance in the marine surface layer. *Boundary-Layer Meteorol* 87(2):233–253. doi:[10.1023/A:1000986130783](https://doi.org/10.1023/A:1000986130783)
- Siqueira M, Katul GG (2002) Estimating heat sources and fluxes in thermally stratified canopy flows using higher-order closure models. *Boundary-Layer Meteorol* 103(1):125–142. doi:[10.1023/A:1014526305879](https://doi.org/10.1023/A:1014526305879)
- Siqueira M, Lai CT, Katul GG (2000) Estimating scalar sources, sinks, and fluxes in a forest canopy using Lagrangian, Eulerian, and hybrid inverse models. *J Geophys Res* 105:29475–29488. doi:[10.1029/2000JD900543](https://doi.org/10.1029/2000JD900543)
- Sirivat A, Warhaft Z (1982) The mixing of passive helium and temperature fluctuations in grid turbulence. *J Fluid Mech* 120:475–504. doi:[10.1017/S0022112082002869](https://doi.org/10.1017/S0022112082002869)
- Sorbjan Z (ed) (1989) *Structure of the atmospheric boundary layer*. Prentice Hall, Englewood Cliffs, 317 pp
- Stull R (1988) *An introduction to boundary layer meteorology*. Kluwer Academic Press, Dordrecht, 666 pp
- Thomas C, Martin JC, Goeckede M, Siqueira MB, Foken T, Law BE et al (2008) Estimating daytime sub-canopy respiration from conditional sampling methods applied to multi-scalar high frequency turbulence time series. *Agric Meteorol* 148:1210–1229. doi:[10.1016/j.agrformet.2008.03.002](https://doi.org/10.1016/j.agrformet.2008.03.002)
- Warhaft Z (1981) The use of dual heat injection to infer scalar covariance decay in grid turbulence. *J Fluid Mech* 104:93–109. doi:[10.1017/S0022112081002838](https://doi.org/10.1017/S0022112081002838)
- Wesely ML (1976) Combined effect of temperature and humidity fluctuations on refractive index. *J Appl Meteorol* 15:43–49. doi:[10.1175/1520-0450\(1976\)015<0043:TCEOTA>2.0.CO;2](https://doi.org/10.1175/1520-0450(1976)015<0043:TCEOTA>2.0.CO;2)
- Williams CA, Scanlon TM, Albertson JD (2007) Influence of surface heterogeneity on scalar dissimilarity in the roughness sublayer. *Boundary-Layer Meteorol* 122(1):149–165. doi:[10.1007/s10546-006-9097-x](https://doi.org/10.1007/s10546-006-9097-x)
- Wyngaard JC, Pennel WT, Lenschow DH, LeMone MA (1978) The temperature-humidity covariance budget in the convective boundary layer. *J Atmos Sci* 58:35–47